

## Implantation-induced amorphization of InP characterized with perturbed angular correlation

E. Bezakova, A. P. Byrne, C. J. Glover, M. C. Ridgway, and R. Vianden

Citation: *Appl. Phys. Lett.* **75**, 1923 (1999); doi: 10.1063/1.124872

View online: <https://doi.org/10.1063/1.124872>

View Table of Contents: <http://aip.scitation.org/toc/apl/75/13>

Published by the [American Institute of Physics](#)

---

---

**AIP** | Conference Proceedings

Get **30% off** all  
print proceedings!

Enter Promotion Code **PDF30** at checkout



# Implantation-induced amorphization of InP characterized with perturbed angular correlation

E. Bezakova

*Department of Nuclear Physics, Research School of Physical Sciences and Engineering, Australian National University, Canberra, Australia*

A. P. Byrne

*Department of Nuclear Physics Research School of Physical Sciences and Engineering and Department of Physics, The Faculties, Australian National University, Canberra, Australia*

C. J. Glover and M. C. Ridgway<sup>a)</sup>

*Department of Electronic Materials Engineering, Research School of Physical Sciences and Engineering, Australian National University, Canberra, Australia*

R. Vianden

*Institut fuer Strahlen-und Kernphysik, Universitat Bonn, Bonn, Germany*

(Received 27 April 1999; accepted for publication 2 August 1999)

The perturbed angular correlation (PAC) technique has been used to characterize the implantation-induced crystalline-to-amorphous transformation in InP. Radioactive  $^{111}\text{In}$  probes were first introduced in InP substrates which were then irradiated with Ge ions over an ion-dose range extending 2 orders of magnitude beyond that required for amorphization. Crystalline, disordered and amorphous probe environments were subsequently identified with PAC. The dose dependence of the relative fractions of the individual probe environments were determined, a direct amorphization process consistent with the overlap model was quantified and evidence for a second amorphization process via the overlap of disordered regions was observed. Given the ability to differentiate disordered and amorphous probe environments, a greater effective resolution was achieved with the PAC technique compared with other common analytical methodologies. © 1999 American Institute of Physics. [S0003-6951(99)02639-X]

Ion implantation has multiple applications in InP-based device fabrication and thus, a further understanding of irradiation-induced disorder production is of both scientific and technological significance. In previous studies, the crystalline-to-amorphous transformation has been extensively characterized with Rutherford backscattering spectrometry/channeling (RBS/C)<sup>1</sup> and the influences of ion mass, ion dose, ion-dose rate and implantation temperature have been well established. A variety of models for the amorphization process have been proposed<sup>2-7</sup> and RBS/C measurements of the relative concentration of *displaced* lattice atoms have commonly been used to validate such theoretical predictions. Note however that the displaced-lattice-atom calculation includes point defects, defect complexes and amorphous clusters and thus, necessarily overestimates the *amorphous* fraction. Other methodologies such as optical absorption<sup>1</sup> similarly measure the superposition of defect configurations. For the present report, the crystalline-to-amorphous transformation in ion-implanted InP has been characterized with the perturbed angular correlation (PAC) technique.<sup>8</sup> Measurements have been compared with theoretical models and correlated with RBS/C and transmission electron microscopy results. As demonstrated below, multiple atomic-scale environments of an interacting probe atom

have been identified and hence, a greater effective resolution was attainable with PAC relative to the alternative analytical methodologies listed above.

In general, PAC is sensitive to the local atomic environment about a radioactive probe atom through the interaction of the probe nuclear quadrupole moment of an intermediate nuclear state and the local electric field gradient (EFG) produced by the substrate lattice. As a consequence of this interaction, the angular correlation of the two  $\gamma$  rays associated with the intermediate state is altered, yielding a modulation of the spectrum dependent on the time spent in the intermediate state. Deviations from cubic lattice symmetry due to implantation-induced disorder result in an EFG and hence, PAC can yield information on defects in close proximity to the probe and displacements of the probe relative to an unperturbed location. Although PAC has been utilized previously to characterize defects and/or dopant activation in compound semiconductors,<sup>9</sup> the radioactive probe was typically an ion-implanted *impurity*, able to complex with impurity-specific defects. Herein, the probe was a *lattice* constituent in a cubic environment prior to ion irradiation and as a consequence, represents a unique application of the PAC technique to characterize *lattice* disorder in ion-implanted InP.

Radioactive  $^{111}\text{In}$  probes were introduced in semi-insulating InP substrates of (100) orientation by a direct-production/recoil-implantation methodology as shown schematically in Fig. 1 and described in Ref. 10. A Rh foil of thickness  $\sim 2.5 \mu\text{m}$  was irradiated with  $^{12}\text{C}$  ions of energy

<sup>a)</sup> Author to whom correspondence should be addressed.  
Electronic mail: mcr109@rsphysse.anu.edu.au

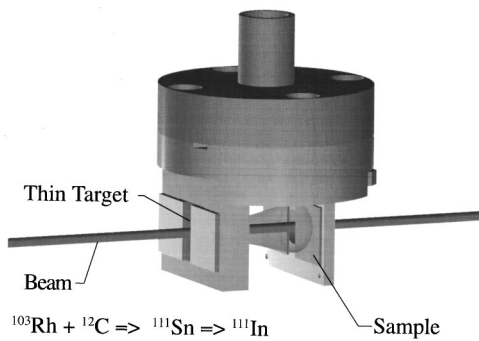


FIG. 1. Schematic diagram of the direct-production/recoil-implantation methodology.

$^{69}\text{MeV}$  and  $^{111}\text{In}$  isotopes were produced via the  $^{103}\text{Rh}(^{12}\text{C},p3n)^{111}\text{Sn}$  and  $^{103}\text{Rh}(^{12}\text{C},4n)^{111}\text{Sb}$  reactions. The calculated angular distributions of the recoiled and transmitted reaction products were significantly broader than that of the scattered and transmitted  $^{12}\text{C}$  ions.<sup>11</sup> InP substrates were thus positioned behind the Rh foil and offset from the incident ion-beam direction such that  $\sim 60\%$  of the recoiled and transmitted reaction products were implanted in the substrate (with an average energy of 4 MeV) while the introduction of  $^{12}\text{C}$  was negligible. For the geometrical conditions utilized herein, the radioactive probe concentration within the InP substrates was approximately uniform over depths of  $\sim 0.5\text{--}2.0\ \mu\text{m}$ . An  $800^\circ\text{C}/10\ \text{s}$  rapid thermal annealing cycle, with proximity capping and an  $\text{N}_2$  ambient, was then utilized to remove recoil-implantation-induced disorder and ensure the  $^{111}\text{In}$  probes occupied substitutional lattice positions. The  $^{111}\text{In}$  areal concentration was  $\sim 1.3 \times 10^{10}/\text{cm}^2$ .

Radioactive InP substrates were then implanted at temperatures of  $\sim -196^\circ\text{C}$  with  $^{74}\text{Ge}$  ions, utilizing a multiple energy (1.0, 2.0, 3.5, and 6.8 MeV), multiple dose ( $2.0 \times 10^{11}$ ,  $2.7 \times 10^{11}$ ,  $4.0 \times 10^{11}$ , and  $1.1 \times 10^{12}/\text{cm}^2$  and multiples thereof) implantation sequence, to produce a near-constant distribution of energy deposited in vacancy production over depths of  $\sim 0.2\text{--}2.5\ \mu\text{m}$ .<sup>11</sup> PAC measurements were then performed at room temperature utilizing a coplanar array of four conically shaped  $\text{BaF}_2$  detectors with a time resolution of  $\sim 550\ \text{ps}$ , sufficient for measuring transition frequencies of  $\leq 1000\ \text{MHz}$ . Samples were positioned perpendicular to the detector plane and at  $45^\circ$  with respect to the detectors. The ratio function  $R(t)$ , or equivalently, the product of the perturbation function [ $G_{22}(t)$ ] and effective anisotropy coefficient ( $A_{22}^{\text{eff}}$ ), was determined from delayed coincidence spectra collected over a  $\sim 10\ \text{h}$  period. Given the presence of nonunique EFGs as discussed below, subsequent analysis was performed assuming a polycrystalline material. The validity of this assumption was confirmed given the  $R(t)$  spectra converged asymptotically to the hardcore value of a powder source.<sup>8</sup>

Figure 2 shows  $R(t)$  spectra of implanted InP as a function of total ion dose. Note that the unimplanted sample spectrum exhibited no time dependence, indicative of the lack of recoil-implantation-induced disorder over the extent of the  $^{111}\text{In}$  probe distribution. In contrast, a dose-dependent rise time was apparent in the implanted sample spectra, which converged at the hardcore value of  $\sim -0.019$  for times in excess of  $\sim 300\ \text{ns}$  (for doses  $> 2 \times 10^{12}/\text{cm}^2$ ). The

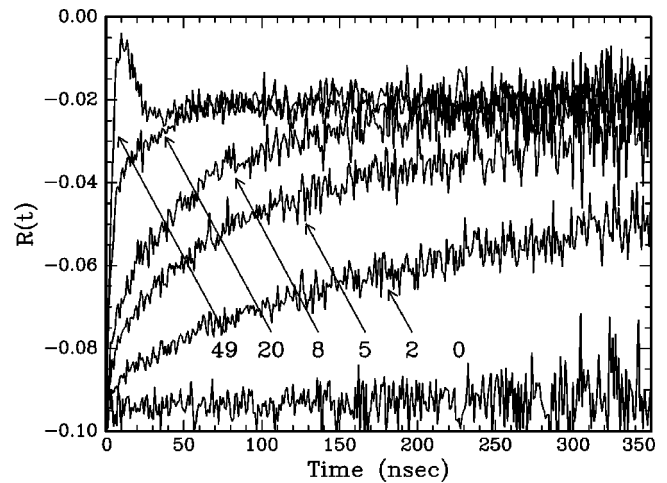


FIG. 2. Ratio functions for Ge-implanted InP samples as a function of ion dose. Numbers on the figure indicate the total Ge dose in units of  $1 \times 10^{12}/\text{cm}^2$ .

observed  $R(t)$  time dependence was consistent with the presence of a nonunique EFG or equivalently, multiple perturbative sources. However, two distinct frequency distributions (assumed Lorentzian), with mean frequencies  $\omega_1$  and  $\omega_2$  ( $15.4 \pm 0.3$  and  $197.3 \pm 2.2\ \text{MHz}$ , respectively) and widths  $\delta_1$  and  $\delta_2$  ( $24.2 \pm 0.6$  and  $69.0 \pm 2.0\ \text{MHz}$ , respectively) were apparent following Fourier transformation. Accordingly, the PAC spectra were analyzed with a two-fraction perturbation function of the form:

$$G_{22}(t) = f_1 G_{22}(\omega_1, t) + f_2 G_{22}(\omega_2, t), \quad (1)$$

where  $f_1 + f_2 = 1$  and the implanted  $^{111}\text{In}$  probes were thus considered to occupy one of two possible environments—disordered ( $f_1$ ) or amorphous ( $f_2$ ).<sup>12</sup> For doses  $\leq 2 \times 10^{12}/\text{cm}^2$ , a third component  $f_3$  equivalent to an unperturbed site was also incorporated. In contrast, only a single component equivalent to an amorphous environment ( $f_2 = 1$ ) was necessary for ion doses greater than that required for amorphization ( $\sim 49 \times 10^{12}/\text{cm}^2$ ) as confirmed from RBS/C measurements (not shown). As anticipated, greater values of both  $\omega$  and  $\delta$  were observed for a probe in an amorphous environment relative to that on a lesser perturbed site. Comparable numbers have been reported for the former in other amorphous materials.<sup>13</sup>

Figure 3 shows the amorphous fraction  $f_2$  determined from PAC measurements as a function of ion dose including comparisons with the overlap model<sup>2,3</sup> wherein

$$f_2 = 1 - \sum_{k=0}^m [(AD)^k / k!] e^{-AD}, \quad (2)$$

where  $A$  is the area damaged by a single ion,  $D$  is the ion dose, and  $m$  is the number of overlaps required for amorphization. For the implantation conditions utilized herein, amorphization evidently proceeded directly from individual collision cascades or equivalently, the overlap of disordered regions was not required. A value of  $(4.2 \pm 0.2) \times 10^{-14}\ \text{cm}^2$  was calculated for  $A$ , the area amorphized at the cascade core. In recent RBS/C measurements,<sup>1</sup>  $A$  values reported therein for an ion of comparable mass (Se) exceeded those of the present study by a factor of  $\sim 2.6$  as potentially attribut-

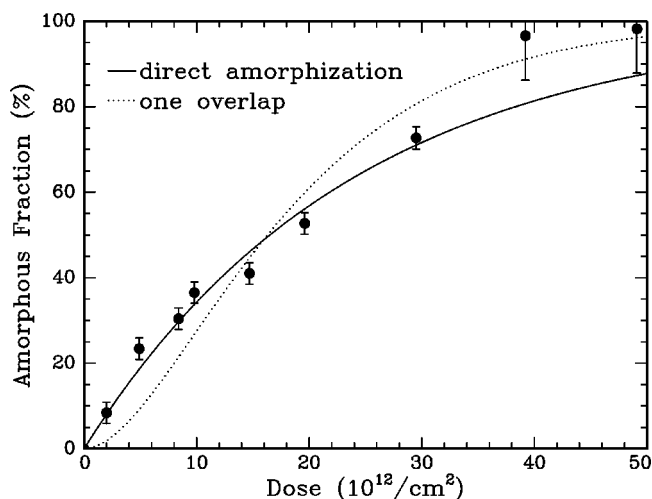


FIG. 3. Amorphous fraction determined with PAC for Ge-implanted InP samples as a function of ion dose.

able to the previously described overestimation of the amorphous fraction inherent with the RBS/C technique.

From Fig. 3, a second possible amorphization mechanism was identified for the dose range  $> \sim 30 \times 10^{12}/\text{cm}^2$ . Therein, damage production was evidently more efficient than predicted for direct amorphization as attributed to the additional contribution of the overlap of two or more disordered regions. (Note that the probability for overlap was necessarily greatest as the dose approached the amorphization threshold.) This supposition was consistent with *in situ* transmission electron microscopy observations where two amorphization processes have been identified in Si-implanted InP: Zheng *et al.*<sup>14</sup> observed direct amorphization in the cascade core, as described above, and also, a strain-driven collapse to a second amorphous structure in an area of critical size separating three ion impacts. The results presented in Fig. 3 were thus also compared with the composite model,<sup>4</sup> which includes both direct and overlap amorphization mechanisms, although significant improvements were not achieved. Subsequent comparisons with alternative models were less satisfactory.

The physical significance of the magnitude of  $A$ , equivalent to an area of radius 4–5 interatomic distances amorphized at the cascade core, warrants further consideration. As noted previously by Cohen *et al.*,<sup>15</sup> radii of considerably lesser values would be physically meaningless given a minimum size requirement over which to define the amorphous phase within a crystalline lattice. Although amorphous InP lacks long-range order, the basic tetragonal bonding structure or short-range order characteristic of crystalline material is, in general, retained.<sup>16,17</sup> However, a multitude of interatomic configurations have been theoretically predicted<sup>16</sup> and/or experimentally confirmed<sup>17</sup> including coordination numbers ranging from three to six atoms and a degree of homopolar bonding for both lattice constituents. In general, the EFG in an amorphous material is determined predominantly by the nearest neighbor<sup>18</sup> which in amorphous InP thus includes a significant fraction of homopolar-bonded In atoms. Though not shown in Fig. 2, PAC measurements were also performed on samples irradiated over an ion-dose range extend-

ing two orders of magnitude greater than that required for amorphization. While no significant differences were observed in the  $R(t)$  spectra, an ion-dose dependence for the amorphous-phase structure cannot be discounted given the amorphous environment identified with PAC was potentially representative of the superposition of the multiple, theoretically predicted interatomic configurations. Subtle, dose-dependent changes in the relative fractions of such configurations may not be resolvable with this technique.

In conclusion, a methodology for the production and introduction of radioactive  $^{111}\text{In}$  probes was developed and thereafter, the crystalline-to-amorphous transformation in ion-implanted InP was characterized with PAC. Crystalline, disordered, and amorphous environments of the radioactive probe have been identified and thus, a greater effective resolution was achieved with PAC compared with other common analytical techniques. The dose dependence of the relative fractions of the individual probe environments were determined, a direct amorphization process consistent with the overlap model was quantified and for the dose range approaching the amorphization threshold, evidence of a second amorphization process via the overlap of disordered regions has been observed.

M.C.R. thanks H. Bernas for helpful discussions. A.P.B. and M.C.R. were supported by the Australian Bilateral Science and Technology Program and R.V. was supported by D.L.R. under Contract No. AUS-014-96.

<sup>1</sup>E. Wendler, T. Opfermann, and P. I. Gaiduk, *J. Appl. Phys.* **82**, 5965 (1997), and references therein.

<sup>2</sup>J. F. Gibbons, *Proc. IEEE* **60**, 1062 (1972).

<sup>3</sup>D. A. Thompson, A. Golanski, K. H. Haugen, D. V. Stevanovic, G. Carter, and C. E. Christodoulides, *Radiat. Eff.* **52**, 69 (1980).

<sup>4</sup>J. R. Dennis and E. B. Hale, *J. Appl. Phys.* **49**, 1119 (1978).

<sup>5</sup>G. Carter and R. Webb, *Radiat. Eff.* **43**, 19 (1979).

<sup>6</sup>N. Hecking, K. F. Heidemann, and E. Te Kaat, *Nucl. Instrum. Methods Phys. Res. B* **15**, 760 (1986).

<sup>7</sup>S. U. Campisano, S. Coffa, V. Raineri, F. Priolo, and E. Rimini, *Nucl. Instrum. Methods Phys. Res. B* **80/81**, 514 (1993).

<sup>8</sup>H. Frauenfelder and R. M. Steffen, in *Alpha, Beta and Gamma Ray Spectroscopy*, edited by K. Seigbahn (North Holland, Amsterdam, 1968) p. 997.

<sup>9</sup>D. Forkel-Wirth, *Nucl. Instrum. Methods Phys. Res. B* **126**, 396 (1997) and references therein.

<sup>10</sup>E. Bezakova, Ph.D. thesis, Australian National University, Canberra, 1998.

<sup>11</sup>J. F. Ziegler, J. P. Biersack, and U. Littmark, *The Stopping and Range of Ions in Matter* (Pergamon, Oxford, 1985).

<sup>12</sup>The “disordered” or weakly disturbed environment resulted from a random distribution of defects, located within several interatomic distances from the radioactive probe, with low interaction frequencies that yielded small EFGs. In contrast, the “amorphous” or highly disturbed environment was manifested by high interaction frequencies, large EFGs and the rapid convergence to the hard core value. The PAC spectrum for the latter was characteristic of a high frequency distribution of significant width—periodic modulations were not observed for times greater than  $\sim 15$  ns due to the convolution of the multiple frequencies.

<sup>13</sup>L. A. Mendoza-Zelis, L. C. Damonde, A. G. Bibiloni, J. Desimoni, and A. R. Lopez-Garcia, *Phys. Rev. B* **34**, 2982 (1986).

<sup>14</sup>P. Zheng, M.-O. Ruault, O. Kaitasov, J. Crestou, B. Descouts, P. Krauz, and N. Duhamel, *J. Phys. D* **23**, 877 (1990).

<sup>15</sup>C. Cohen, A. Benyagoub, H. Bernas, J. Chaumont, L. Thome, M. Berti, and A. V. Drigo, *Phys. Rev. B* **31**, 5 (1985).

<sup>16</sup>L. J. Lewis, A. De Vita, and R. Car, *Phys. Rev. B* **57**, 1594 (1998).

<sup>17</sup>C. J. Glover, M. C. Ridgway, K. M. Yu, G. J. Foran, T. W. Lee, Y. Moon, and E. Yoon, *Appl. Phys. Lett.* **74**, 1713 (1999).

<sup>18</sup>P. Panissod, I. Bakonyi, and R. Hasegawa, *Phys. Rev. B* **28**, 2374 (1983).